Second Conference on Smart Monitoring,
Assessment and Rehabilitation of Civil Structures

SMAR 2013

# Experimental evaluation of FRP-to-concrete bond strength in EBROG technique for strengthening concrete members

Ardalan Hosseini[1] and Davood Mostofinejad[2]

[1] Graduate Student, Civil Engineering Department, Isfahan University of Technology (IUT), Isfahan, Iran
[2] Professor, Civil Engineering Department, Isfahan University of Technology (IUT), Isfahan, Iran

ABSTRACT: Bond strength of fiber reinforced polymer (FRP) to concrete substrate is the most important factor controlling debonding failure mechanisms of various forms in externally strengthened concrete members utilizing FRP composites. Externally bonded reinforcement on grooves (EBROG) technique has been recently introduced as a promising alternative to externally bonded reinforcement (EBR) method to postpone or, in some cases, fully eliminate debonding failure in FRP strengthened RC beams. Due to the novelty of the EBROG technique, only few studies have been conducted up to now on utilizing the technique in flexural/shear strengthening of RC beams. Consequently, the main intention of the current study is to experimentally evaluate FRP-to-concrete bond capacity in EBROG technique by means of single-shear bond tests. To do so, eight concrete prism specimens were externally strengthened with carbon fiber reinforced polymer (CFRP) sheets utilizing EBROG and the conventional EBR techniques, and were subjected to single-shear test. The results showed that EBROG technique operates much more effective than conventional EBR technique in transmission of interfacial shear stresses from FRP composite to concrete substrate.

## 1 INTRODUCTION

In the last few years, fiber reinforced polymers (FRPs) have attracted lots of interest as an alternative to conventional materials for strengthening of existing reinforced concrete (RC) structures. Certain advantages of FRP composites including high strength, light-weight, and ease of application lead engineers to use FRP composites in strengthening projects worldwide (ACI 440.2R-08). Externally bonding of FRPs to the concrete face of RC beams and slabs has been utilized to improve flexural/shear behavior of the members. The most common technique for strengthening of RC members is externally bonded reinforcement (EBR) method which can reduce the project cost due to ease of application; however, the technique suffers from undesirable failure mechanism, i.e. debonding. Premature debonding of the FRP composite from the concrete substrate results an undesirable brittle failure mode which occurs before reaching the whole tensile capacity of the composite. Except sufficiently anchored FRP systems, debonding failure mechanisms of various forms are unavoidable in FRP strengthened RC beams using EBR technique (Yao et al., 2005). Consequently, strengthening guidelines such as ACI 440.2R-08 limit strain value in FRP reinforcements to the strain level at which debonding may occur.

## 2 EBROG TECHNIQUE

Externally bonded reinforcement on grooves (EBROG) technique has been recently introduced by Mostofinejad & Mahmoudabadi (2010). The technique is consisted of cutting grooves into the tension face of concrete beams, filling them with proper epoxy resin, and bonding FRP sheets on the member's surface over the filled grooves. Among different grooves' configurations including transverse, diagonal and longitudinal grooves, cutting 3 longitudinal grooves having 3 × 10 mm (width × depth) dimensions was reported to completely eliminate debonding of CFRP sheets from small-scale concrete beam specimens and increase the ultimate loads up to 80 % compared with conventional EBR strengthened specimens. Furthermore, costly surface preparation in EBR method was completely eliminated when using EBROG technique.

Performance of EBROG method for flexural strengthening of RC beams was more investigated by Mostofinejad et al. (2012). They investigated the effect of multilayer FRP strengthening on flexural behavior of RC beams. Based on their experimental results, in EBROG technique due to more contact between FRP sheet and concrete surface and also penetration of stress transfer to deeper layers of concrete, debonding failure is completely eliminated and the most probable failure mode in strengthened beams is FRP rupture, or in some cases, concrete cover separation.

More recently, Mostofinejad & Tabatabaei Kashani (2013) investigated the effect of EBROG technique as an alternative to EBR method for shear strengthening of RC beams. Mostofinejad & Tabatabaei Kashani (2013) reported that, using EBROG technique prior to shear strengthening of RC beams by CFRP sheets can change the failure mode from shear to flexural and increase ultimate load capacity of the beams up to 15 % compared to EBR strengthened specimens. This is while no debonding was reported in CFRP shear reinforcements.

In both EBR and EBROG techniques, FRP-to-concrete bond strength plays an important role in recognition of flexural/shear behavior of RC strengthened members and, subsequently, affects all strengthening calculations. As a consequence, the main intension of the current study is to compare the bond strength of CFRP sheets attached to concrete surface using EBR and EBROG techniques by means of single-shear bond tests on eight concrete prism specimens.

## 3 EXPERIMENTAL PROGRAM

### *3.1 Specimens' characteristics and testing materials*

Experimental program of the current study consisted of eight single-shear tests on concrete prism specimens with dimensions of 150 × 150 × 350 mm (width × height × length). In order to evaluate the bond capacity of CFRP sheets attached to concrete surface using EBROG method, four out of eight specimens were strengthened using EBROG technique. The other four specimens were externally strengthened using the conventional EBR technique for comparison purposes. The main factors considered in the current study included strengthening method and FRP bond length ($L_{FRP}$), while all other experimental parameters remained constant. The notation of test specimens is M-*x*-*n*, in which M refers to strengthening method including EBR or EBROG methods; *x* represents $L_{FRP}$ in mm (75 or 150); and *n* identifies the ordinal number of each test (1 or 2).

In the current experimental program, CFRP sheets were fabricated through wet layup process and were made up of unidirectional carbon fibers manufactured by Sika group. Furthermore, two-component epoxy adhesive, i.e. Sikadur 330 was used for adhering carbon fibers to the concrete substrate, based on the manufacturer suggestion. Mechanical properties of the carbon fibers and the utilized adhesive are provided in Table 1. Note that ancillary tests based on

ASTM D3039 were conducted by the authors to evaluate tensile strength of the carbon fibers. The results showed that the average tensile strength of utilized carbon fibers, fabricated via wet layup process, is equal to 2795 MPa.

Table 1. Properties of FRP materials

| | Type | Thickness (mm) | Tensile strength (MPa) | Elastic modulus (GPa) | Elongation at break (%) |
|---|---|---|---|---|---|
| Fibers | SikaWrap 230C | 0.131 | 4300 | 238 | 1.8 |
| Adhesive | Sikadur 330 | 0.5-0.9 | 30 | 4.5 | 1.5 |

### *3.2 Strengthening procedure*

As mentioned earlier, two strengthening techniques, i.e. EBR and EBROG methods were used to adhere CFRP sheets to the concrete surface of the specimens. Hence, the effect of EBROG technique on FRP-to-concrete bond capacity could be investigated by comparing the results of EBR and EBROG specimens. To strengthen EBR specimens, firs the weak layer of the concrete surface was removed using a grinding machine, and the prepared surface was properly cleaned with air jet. At the end, carbon fibers were cut into selected sizes and were adhered to the concrete surface using Sikadur 330 epoxy adhesive.

Unlike the EBR method, traditional surface preparation was completely eliminated in EBROG technique. To strengthen EBROG specimens, two 5 × 10 mm (width × depth) grooves were cut into the surface of each prism specimen (Figure 1a). Internal side-to-side distance of the grooves was equal to 20 mm, and the grooves length was equal to $L_{FRP}$, i.e. 75 mm or 150 mm. The grooves were then cleaned with air jet and were fully filled using Sikadur 330 epoxy resin (Figure 1b). Immediately after, carbon fiber sheets with selected sizes were bonded on the concrete surface over the grooves. All the strengthened specimens were cured for 7 days in laboratorial condition before testing.

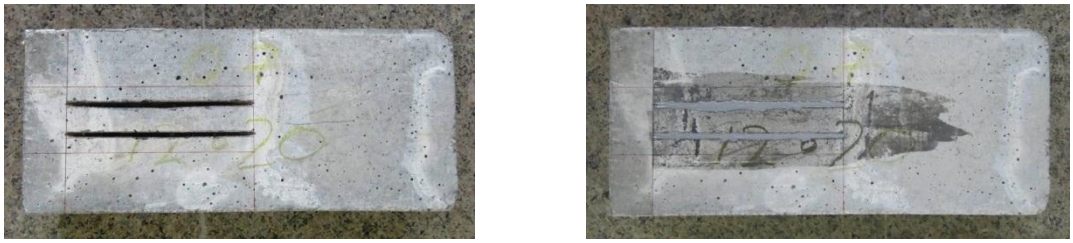

(a) (b)

Figure 1. EBROG technique; a) cutting longitudinal grooves; b) filling the grooves using epoxy adhesive.

### *3.3 Test setup*

In order to investigate FRP-to-concrete bond capacity of test specimens, all EBR and EBROG specimens were subjected to single-shear bond test by means of a 300 kN hydraulic jack designed in the structural lab of Isfahan University of Technology (IUT). Special setup including steel supports was designed and manufactured for single-shear bond tests. Loading arrangement and specimen dimensions are shown in Figure 2a. As illustrated in Figure 2a, an unbonded zone equal to 35 mm, was introduced to the CFRP sheets in order to eliminate stress concentration at the loaded edge of the concrete specimens, based on Mazzotti et al. (2008) investigations.

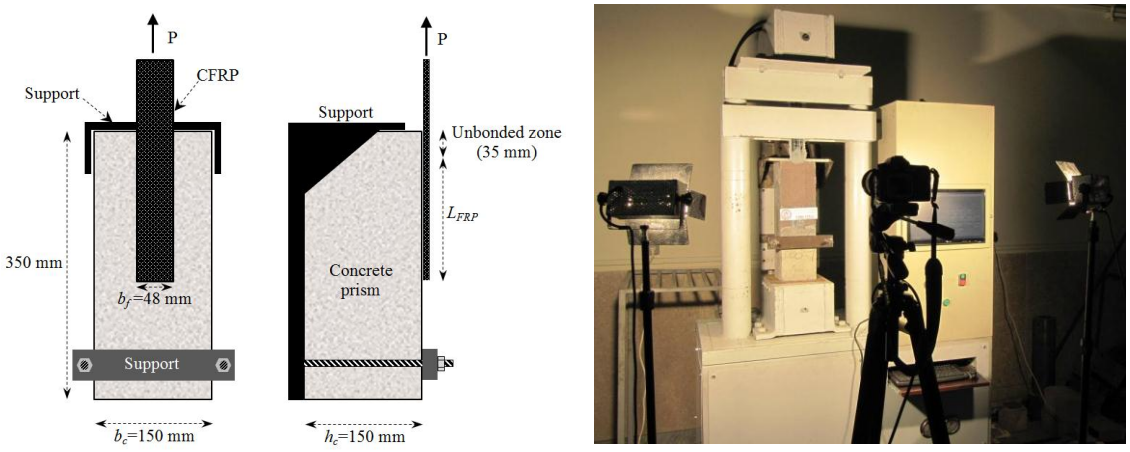


(a) (b)

Figure 2. a) Testing arrangement and specimen dimensions; b) tension machine and test setup.

All tests were performed displacement controlled with a speed of 2.0 mm/min. Furthermore, deformations of the test specimens were considered to be evaluated by means of digital image analysis technique. Consequently, a Nikon D80 digital camera with resolution of 10.0 megapixels (3872 × 2592 pixels) was placed perpendicular to the specimen's face at a distance of 1.0 m. Successive digital images were automatically taken from each specimen undergoing deformation at regular intervals, and a digital data logger was used to monitor the load cell and image numbers, simultaneously. As illustrated in Figure 2b, the specimen's face was illuminated using two white light projectors, in order to eliminate probable parasitic light noises. It should be noted that, a proper texture is necessary for the images to create features upon which image processing can properly operate. As a consequence, a mixture of different colored fine sand was prepared and embedded to the specimens' faces just after end of strengthening process and before epoxy hardening.

## 4 RESULTS AND DISCUSSIONS

### *4.1 Bond strength*

Ultimate loads ($P_{exp}$) of all tested specimens are provided in Table 2. Furthermore, average ultimate loads ($P_{exp,avg}$) corresponding to each pair of identical tests are also calculated and presented in Table 2. The FRP-to-concrete bond strength is considerably increased in EBROG specimens; since the average ultimate loads of EBROG specimens with 75 mm and 150 mm bond length were increased up to 52.5 % and 58.6 %, respectively compared with corresponding EBR specimens. Moreover, theoretical debonding loads ($P_{model}$) corresponding to EBR specimens were calculated from Equation (1), based on Seracino et al. (2007) model, and the results are provided in Table 2.

$$P_{model} = 0.85\left(\frac{d_f}{b_f}\right)^{0.25}(f_c)^{0.33}\sqrt{L_{per}E_fA_f} \quad (1)$$

where $d_f$ and $b_f$ are thickness of the failure plane perpendicular to the concrete surface, and width of FRP strip, respectively; $f_c$ is mean cylindrical compressive strength of concrete; $L_{per}$ is length of the debonding failure plane which can be assumed as $2d_f + b_f$. $E_f$ and $A_f$ are elasticity modulus and transversal area of FRP reinforcement, respectively. Comparing the experimental results of the EBR specimens with predictions of Seracino et al. (2007) model, clearly verifies

the capability of the model in accurate and safe prediction of debonding loads for EBR strengthened specimens, since the average discrepancy between experimental and predicted debonding loads is equal to 3.3 %.

Table 2. Test results

| Test specimen | $f_c$ (MPa) | $L_{FRP}$ (mm) | Failure mode | $P_{exp}$ (kN) | $P_{exp,avg}$ (kN) | Increase in ultimate load (%) | $P_{model}$ (kN) |
|---|---|---|---|---|---|---|---|
| EBR-75-1 | 36.5 | 75 | debonding | 9.52 | 9.66 | - | 9.16 |
| EBR-75-2 | 36.5 | 75 | debonding | 9.80 | | | |
| EBROG-75-1 | 36.5 | 75 | FRP rupture | 14.42 | 14.73 | 52.5 | N.A |
| EBROG-75-2 | 36.5 | 75 | FRP rupture | 15.03 | | | |
| EBR-150-1 | 39.1 | 150 | debonding | 9.42 | 9.51 | - | 9.37 |
| EBR-150-2 | 39.1 | 150 | debonding | 9.60 | | | |
| EBROG-150-1 | 39.1 | 150 | FRP rupture | 14.81 | 15.08 | 58.6 | N.A |
| EBROG-150-2 | 39.1 | 150 | FRP rupture | 15.34 | | | |

It can be concluded from the results of Table 2 that, increasing $L_{FRP}$ from 75 mm to 150 mm in EBR specimens, has no effect on the ultimate bond capacity of FRP-to-concrete joints; since there exists an effective bond length ($L_e$) beyond which an extension of the bond length cannot increase the ultimate capacity of the joint (Chen & Teng, 2001). $L_e$ can be calculated from Equation (2) based on Seracino et al. (2007) model.

$$L_e = \frac{\pi}{2\sqrt{\frac{\tau_f L_{per}}{\delta_f E_f A_f}}} \tag{2}$$

where $\tau_f$ and $\delta_f$ are peak interface shear stress and slip beyond which bond stress is zero, respectively. $\tau_f$ and $\delta_f$ can be calculated from the following equations, suggested by Seracino et al. (2007).

$$\tau_f = (0.802 + 0.078\frac{d_f}{b_f})(f_c)^{0.6} \tag{3}$$

$$\delta_f = \frac{0.73}{\tau_f}\left(\frac{d_f}{b_f}\right)^{0.5}(f_c)^{0.67} \tag{4}$$

Note that effective bond lengths were calculated from Equation (2) as 42.3 and 41.5 mm corresponding to EBR-75-1(2) and EBR-150-1(2) specimens, respectively. Hence, as experimental FRP bond lengths ($L_{FRP}$) in EBR specimens are much greater than calculated $L_e$ values, experimental debonding loads of EBR specimens are independent of $L_{FRP}$.

### *4.2 Failure modes*

As presented in Table 2, all EBR specimens failed due to debonding of CFRP sheets from the concrete substrate. In this case, a thin layer of concrete was attached to the debonded CFRP strip, means that the failure plane occurs within the concrete not adhesive layer (Figure 3a). All EBROG specimens, however, failed due to rupture of CFRP sheets. It means that, cutting two 75 mm long grooves can increase the FRP-to-concrete bond such strength that the debonding failure was completely eliminated and the failure was occurred due to rupture of CFRP composite.

(a)

(b)

Figure 3. a) Debonding of CFRP strip from concrete substrate in specimen EBR-150-1; b) CFRP rupture in specimen EBROG-150-1.

As illustrated in Figure 3b, CFRP rupture in EBROG specimens simultaneously occurs in the zone near to the loaded edge of the concrete prism, and in the fixed end of the CFRP strip clamped in the grips.

### *4.3 Deformation measurement using digital image analysis*

In order to evaluate the relative displacement between the CFRP sheet and concrete substrate during the test process, successive digital images were analyzed using GeoPIV8 software developed by White & Take (2002) at Cambridge University. As detailed discussion on the image analysis technique is beyond the scope of the current study, the readers are referred to White et al. (2003) for further details. Note that capability of the technique in accurate deformation measurements has been previously discussed by Hosseini et al. (2012).

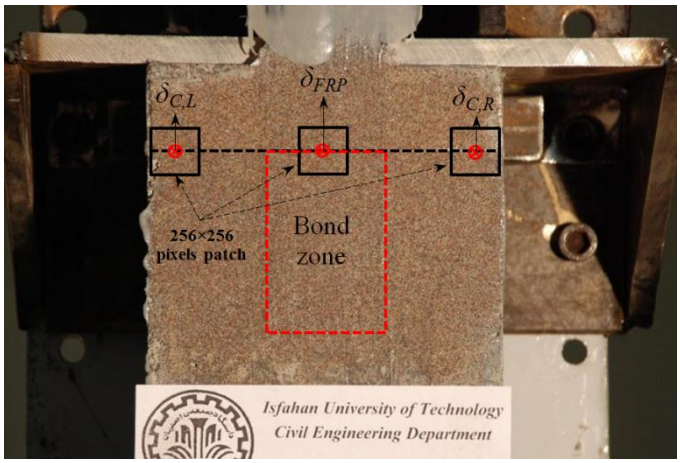


Figure 4. Specimen EBROG-75-1, camera view and locations of 256 × 256 pixels patches.

As illustrated in Figure 4, CFRP deformation, $\delta_{FRP}$, as well as concrete displacements, $\delta_{C,L}$, and $\delta_{C,R}$ corresponding to each digital image were obtained from image analyses by generating 256 × 256 pixels patches. Hence slip values can be calculated from the following equation:

$$s = \delta_{FRP} - (\delta_{C,L} + \delta_{C,R})/2 \quad (5)$$

where $s$ represents slip at loaded end of the CFRP sheet (i.e. the beginning point of the bond length). $\delta_{FRP}$, $\delta_{C,L}$, and $\delta_{C,R}$ are CFRP and concrete deformations, respectively as illustrated in Figure 4. Slip values for each specimen during the test process were calculated from Equation (5) and were used for plotting load-slip curves.

### *4.4 Load-slip behavior*

Load-slip curves for all tested specimens are plotted in Figure 5 in order to better demonstrate the effect of strengthening method on FRP-to-concrete bond behavior. As presented in Figure 5, load-slip behavior of EBR and EBROG specimens are identical up to a load of approximately 7 kN. After the first linear zone of the curves, EBR specimens show a non-linear hardening zone with an increase in load bearing up to 9.5 kN. Finally, the applied load remains approximately constant up to debonding of the CFRP sheet from the concrete substrate. Note that although increasing $L_{FRP}$ has no effect on debonding capacity of EBR specimens; however, increasing the bond length can provide major ultimate slips and results a more ductile failure.

Load-slip behavior of all tested EBROG specimens can be assumed to be bi-linear. Load-slip curves linearly increase up to a load of approximately 9 kN, and then linearly continues upward with a lower stiffness up to the rupture of CFRP sheets around a load of 15 kN. Careful inspection of Figure 5 reveals that the load-slip behavior of EBROG specimens is independent of bond length. This fact can be related to the stronger bond between CFRP composite and the concrete substrate in EBROG method compared with conventional EBR technique.

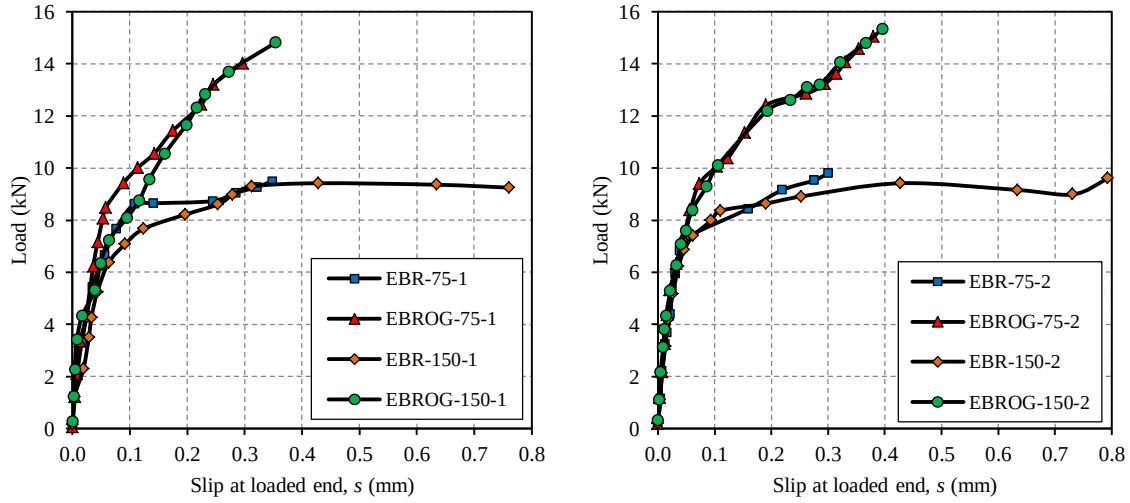


(a) (b)

Figure 5. Load-slip diagrams for testes specimens; a) series 1; b) series 2.

## 5 CONCLUSIONS

FRP-to-concrete bond capacities of EBR and EBROG methods were experimentally evaluated in this paper. Eight single-shear bond tests were conducted on EBR and EBROG specimens and failure loads as well as load-slip diagrams were presented. Based on the experimental results of the current study, the following concluding remarks can be drawn:

- EBROG technique operates much more effective compared to conventional EBR method in transmission of interfacial shear stresses from CFRP composite to concrete substrate; since average bond capacity of EBROG specimens is 55.6 % higher than EBR specimens.
- All EBR specimens failed due to debonding of CFRP sheet from the concrete substrate, while debonding failure was completely eliminated when EBROG technique was used. It means that the whole tensile capacity of the FRP reinforcement could be reached in EBROG specimens.
- Load-slip behavior of EBROG specimens can be assumed to be bi-linear. Although the bond stiffness reduces in the second zone of the curve; however, the load-slip curve linearly continues up to the FRP rupture.
- Seracino et al. bond strength model can accurately predict debonding loads of EBR specimens. However, further experimental and analytical studies are needed to develop an appropriate bond strength model for the EBROG technique.

## 6 REFERENCES

ACI 440.2R. 2008. *Guide for the design and construction of externally bonded FRP systems for strengthening concrete structures*. Farmington Hills, MI.

ASTM D3039/D3039M. 2000. *Standard test method for tensile properties of polymer matrix composites materials*. West Conshohocken, PA.

Chen, JF, and Teng, JG. 2001. Anchorage strength models for FRP and steel plates bonded to concrete. *Journal of Structural Engineering*, ASCE, 127: 784-791.

Hosseini, A, Mostofinejad, D, and Hajialilue-Bonab, M. 2012. Displacement measurement of bending tests using digital image analysis method. *International Journal of Engineering and Technology*, 4: 642-644.

Mazzotti, C, Savoia, M, and Ferracuti, B. 2008. An experimental study on delamination of FRP plates bonded to concrete. *Construction and Building Materials*, 22: 1409-1421.

Mostofinejad, D, Mahmoudabadi, E. 2010. Grooving as alternative method of surface preparation to postpone debonding of FRP laminates in concrete beams. *Journal of Composites for Construction*, ASCE, 14: 804-811.

Mostofinejad, D, Shameli, SM, and Hosseini, A. 2012. Experimental study on the effectiveness of EBROG method for flexural strengthening of RC beams. *Proceedings of the 6th International Conference on FRP composites in Civil Engineering*, CICE2012, Rome, Italy.

Mostofinejad, D, and Tabatabaei Kashani, A. 2013. Experimental study on effect of EBR and EBROG methods on debonding of FRP sheets used for shear strengthening of RC beams. *Composites: Part B*, 45: 1704-1713.

Seracino, R, Raizal Saifulnaz, MR, and Ohlers, DJ. 2007. Generic debonding resistance of EB and NSM plate-to concrete joints. *Journal of Composites for Construction*, ASCE, 11: 62-70.

White, DJ, and Take, WA. 2002. *GeoPIV: Particle Image Velocimetry (PIV) software for use in Getechnical testing*. Cambridge University Engineering Department Technical Report.

White, DJ, Take, WA, and Bolton, MD. 2003. Soil deformation measurement using Particle Image Velocimetry (PIV) and photogrammetry. *Geotechnique*, 53: 619-631.

Yao, J, Teng, JG, and Chen, JF. 2005. Experimental study on FRP-to-concrete bonded joints. *Composites: Part B*, 36: 99-113.